The Astrophysical Journal, 662:1059–1066, 2007 June 20

A STUDY OF THE 3.3 AND 3.4 μm EMISSION FEATURES IN PROTO–PLANETARY NEBULAE[1]

Bruce J. Hrivnak
Department of Physics and Astronomy, Valparaiso University, Valparaiso, IN 46383; bruce.hrivnak@valpo.edu

T. R. Geballe
Gemini Observatory, 670 North A'ohoku Place, Hilo, HI 96720; tgeballe@gemini.edu

and

Sun Kwok
Department of Physics, The University of Hong Kong, Hong Kong, China; and Department of Physics and Astronomy, University of Calgary, Calgary, AB T2N 1N4, Canada; sunkwok@hku.hk
Received 2006 October 13; accepted 2007 March 13

ABSTRACT

Medium-resolution spectra have been obtained of seven carbon-rich proto–planetary nebulae (PPNs) and one young planetary nebula from 3.2 to 3.8 μm, an interval containing the prominent hydrocarbon C—H stretches at 3.3 and 3.4 μm due to aromatic and aliphatic structures, respectively. The 3.3 μm feature is newly identified in IRAS 23304+6147, 22223+4327, and 06530−0213 and is confirmed in Z02229+6208. Three of the PPNs emit in the 3.4 μm feature, two of these being new identifications, IRAS 20000+3239 and 01005+7910, with two others showing possible detections. The 3.3 and 3.4 μm emission features in IRAS 22272+5435 are seen in the nebula offset from the star but not at the position of the central star, consistent with the 2003 results of Goto et al. A similar distribution is seen for the 3.3 μm feature in IRAS 22223+4327. All of the PPNs except IRAS 22272+5435 show Class A 3 μm emission features. These observations, when combined with those of the approximately equal number of other carbon-rich PPNs previously observed, demonstrate that there are large differences in the 3 μm emission bands, even for PPNs with central stars of similar spectral type, and thus that the behavior of the bands does not depend solely on spectral type. We also investigated other possible correlations to help explain these differences. These differences do not depend on the C/O value, since the Class B sources fall within the C/O range found for Class A. All of these 3.3 μm sources also show C_2 absorption and 21 μm emission features, except IRAS 01005+7910, which is the hottest source at B0.

Subject headings: circumstellar matter — infrared: ISM — infrared: stars — ISM: lines and bands — planetary nebulae: general — stars: AGB and post-AGB

1. INTRODUCTION

A family of broad emission features whose strongest members are at 3.3 (3.29), 6.2, 7.7, 8.6, and 11.3 μm (often known as unidentified infrared [UIR] bands) are seen in a variety of objects with strong ultraviolet radiation fields, in particular, H II regions, reflection nebulae, and planetary nebulae (PNs) and in the diffuse interstellar medium. A related set of features at similar wavelengths has been found in some proto–planetary nebulae (PPNs) whose central stars are typically of spectral type F or G and thus have considerably weaker (relative to visible) ultraviolet (UV) fields. In many cases the PPN UIR features are broader and their relative intensities are different from those seen in UV-dominated regions (Geballe 1997). However, in other PPNs the features appear indistinguishable from those seen in UV-dominated regions such as PNs.

As a group, all of the features have been identified as due to C—H or C—C stretching and bending (vibrational) modes of aromatic compounds (Duley & Williams 1981) and are referred to as aromatic infrared bands (AIBs) in the remainder of this paper. Although the general origin of the AIBs is believed to be known, no single compound produces the observed spectrum, and the distribution of compositions of the carriers is unclear, mainly because a wide variety of aromatic compounds produce very similar features. Additional problems include the difficulty in reproducing interstellar conditions in the laboratory, and the frequent constraint that laboratory measurements be made in absorption with the candidate in a solid or semisolid state.

The most generally accepted identifications for the carriers of the AIBs seen in UV-excited regions have been free-floating polycyclic aromatic hydrocarbon (PAH) molecules (Léger & Puget 1984; Allamandola et al. 1989; Puget & Léger 1989) or similar molecules in very small grains made of hydrogenated amorphous carbons (HACs; Duley & Williams 1983), quenched carbonaceous composites (QCCs; Sakata et al. 1984), or coal (Papoular et al. 1996; Guillois et al. 1996; Papoular 2001). There are several reasons (e.g., Allamandola et al. 1989 and references therein), apart from the general spectral agreement between astronomical and laboratory measurements (Léger & Puget 1984), for identifying the carriers as PAH molecules or very small grains rather than standard-size dust particles. First, carbon-rich molecules including PAHs are chemically expected to form in the cooling carbon-rich gas and are stable. Second, the ratios of the AIB intensities suggest that the typical emitters in UV-excited regions are made of several tens of atoms. Third, the emission features often arise in cold environments such as reflection nebulae, and therefore, the carriers that are emitting not only are not in thermal

[1] This research is based on observations made at the W. M. Keck Observatory by Gemini staff, supported by the Gemini Observatory, which is operated by the Association of Universities for Research in Astronomy, Inc., on behalf of the international Gemini partnership of Argentina, Australia, Brazil, Canada, Chile, the United Kingdom, and the United States of America. The W. M. Keck Observatory is operated as a scientific partnership among the California Institute of Technology, the University of California, and the National Aeronautics and Space Administration. The Observatory was made possible by the generous financial support of the W. M. Keck Foundation.

TABLE 1
NIRSPEC Observing Log

IRAS ID	Date	Exposure Time (s)	Seeing[a] (arcsec)	Air Mass	Slit Pos.Angle (deg)	Calibration Star			Observing Notes
						Name	L (mag)	T (K)	
01005+7910	2000 Dec 16	1800	0.7	2.19	270	BS 357 (F5 V)	5.13	6530	1
Z02229+6208	2000 Dec 16	320	0.7	1.50	270	BS 860 (F4 V)	4.55	6600	1
06530−0213	2000 Dec 16	480	0.7	1.19	270	BS 2530 (F2 V)	4.93	6750	1
20000+3239	2001 Jun 12	480	0.8	1.05	...	BS 7550 (F5 V)	6.39	6530	2
22223+4327	2001 Nov 21	480	0.7	1.15	...	HIP 110305 (F5 V)	6.28	6530	3
22272+5435	2001 Nov 21	80	0.7	1.23	...	HIP 110305 (F5 V)	6.28	6530	3
23304+6147	2001 Nov 21	720	0.7	1.35	...	HIP 110305 (F5 V)	6.28	6530	3
21282+5050	2001 Jun 12	1320	0.8	1.18	...	BS 7756 (F5 V)	4.74	6530	2

Notes.—Observing notes: (1) problems with detector window; (2) poor weather, ice; (3) ice, noisy.
[a] Seeing as measured at 2.2 μm.

equilibrium with their environments, but also must have only a modest number of vibrationally excitable modes.

Aliphatic groups, which can be attached to aromatic hydrocarbons such as PAHs and which are present in the above solid-state materials, are believed to be responsible for the 3.4 μm emission feature which frequently accompanies the stronger 3.3 μm AIB feature in PNs, H II regions, and reflection nebulae. They also have received increasing recognition in the past decade as a significant component of carbonaceous interstellar dust. The symmetric and asymmetric C−H stretching modes of $-CH_3$ (methyl) and $-CH_2-$ (methylene) groups in the 3.4–3.5 μm region have been detected in the diffuse interstellar medium (Pendleton et al. 1994), circumstellar envelopes (Geballe et al. 1992), the ejecta from a carbon star (Lequeux & Jourdain de Muizon 1990), external galaxies (Imanishi & Dudley 2000), and meteorites (Pendleton & Allamandola 2002). The aliphatic C−H bending mode at 6.9 μm has been detected in a number of PPNs (Kwok et al. 1999; Hrivnak et al. 2000). The existence of broad infrared emission plateaus in PPNs can also be attributed to the stretching and bending modes of various aliphatic groups (Kwok et al. 2001).

PPNs are a short-lived (few thousand years) late stage of stellar evolution following the end of asymptotic giant branch (AGB) mass loss, in which the star's temperature increases from ~5000 to ~30,000 K, and the star is surrounded by a detached, expanding circumstellar envelope (CSE; Kwok 1993) with a basically bipolar structure (Ueta et al. 2000; Su et al. 2001). AIB features are seen in many PPNs, including ones whose central stars emit little UV radiation. This suggests that the carriers in them cannot be neutral PAHs and must either be ionized PAHs, which can absorb at visible wavelengths (see, e.g., Joblin et al. 1996; Li & Draine 2002), or some other type of hydrocarbon.

In some PPNs the relative strengths of aromatic and aliphatic features differ from those of PNs. In particular, the 3.4 μm feature, which is much weaker than the 3.3 μm feature in UV-excited regions, is of comparable strength in some PPNs (Geballe & van der Veen 1990; Geballe et al. 1992). It is important to note that the spectral shape of the 3.4 μm feature in these PPNs does not resemble the feature in UV-excited regions, and thus the carriers of the 3.4 μm features in these two classes of objects are not identical.

Neither the aromatic nor aliphatic features are seen in the preceding stage of stellar evolution, the AGB stage, although infrared absorption due to C_2H_2 is often present in carbon-rich AGB stars with thick circumstellar envelopes (Volk et al. 2000; Hony et al. 2002). Taken together, the observations suggest an evolution in the carbon chemistry seen in the CSE from absorption due to small hydrocarbon molecules to aliphatic and then to aromatic bands as the stars evolve rapidly from the AGB to PPN to PN stages (Kwok et al. 1999).

In addition to the aromatic and aliphatic features, there are other broad infrared spectral features that are unusually prominent in carbon-rich PPNs. A strong, unidentified emission feature at ~21 μm is found almost exclusively in PPNs (Kwok et al. 1989; Volk et al. 1999). A very broad 30 μm feature has been known for several decades to exist in carbon-rich evolved stars and PNs (Forrest et al. 1981) and has been seen in carbon-rich PPNs, including all of the 21 μm sources (Omont et al. 1995; Hrivnak et al. 2000; Volk et al. 2002). Again, the PPN stage seems to play a key role in the evolution of these features, and it may be that an understanding of any of these infrared features will require an understanding of the relationship between all of them. Thus, the study of molecules and solid-state features in these PPNs may be crucial to an understanding of the carbon-based chemicals that are returned to the ISM from these low- and intermediate-mass stars.

In this paper we present new 3 μm spectra of seven carbon-rich PPNs, several of which had not been previously observed in this wave band. In particular, we examine the presence and strength of the 3.4 μm feature in PPNs in order to determine its properties and to see if there is evidence for a correlation, and thus perhaps an evolution, in the relative strengths of the 3.3 and 3.4 μm features with PPN spectral type. We also crudely explore the spatial variation of the emission features in the nebulae that are resolved. Finally, we also explore the possible correlation of the 3.3 and 3.4 μm emission features with other spectral features, using an essentially complete sample of carbon-rich PPNs.

2. OBSERVATION AND DATA REDUCTION

The observations were carried out at various times during 2000 and 2001 with the facility infrared spectrograph NIRSPEC (McLean et al. 1998) on the 10 m Keck II telescope on Mauna Kea as part of a program of limited access to NIRSPEC on Keck provided to the Gemini Observatory community during 2000–2001. NIRSPEC uses an Aladdin 1024 × 1024 pixel InSb array. Its low-resolution grating mode was used with a 3 pixel (0.57″) wide slit and a spectral resolution of ~2000. The spectra we obtained extend from 3.0 to 3.8 μm. The telescope was nodded 21″ along the slit, which had a length of 42″. Spectra typically were extracted from eight adjacent rows (1.5″). An observing log is given in Table 1.

The various observing runs each encountered some difficulties that affected the quality of the data. In the 2000 December

observing run the data were corrupted somewhat by transient dust and defects on the NIRSPEC dewar window, which produced spurious bands (i.e., spectra) of bright continuum on the array. During this run, the slit was rotated to compensate for field rotation to maintain an east–west slit orientation, resulting in the contaminating continuum signal occurring at various locations on the array that changed with time. In subsequent runs the slit was physically fixed in place to reduce this effect, but with the result that its orientation on the sky varied from object to object and during each measurement. Thus, no slit orientations are given for the 2001 measurements. Weather conditions were marginal during the 2001 June run. During the 2001 June and November observing runs, water ice frozen on the optical surface inside NIRSPEC produced strong absorption shortward of 3.2 μm. Because the ice layer was nonuniform and the comparison star was not observed at exactly the same position on the detector, the ratioed spectra show uncanceled ice features shortward of 3.2 μm, and in many cases, this portion of the spectrum is unusable.

All spectra were extracted from the co-added subtracted pairs of spectral images. Those of the PPNs were ratioed by the spectra of the calibration stars listed in Table 1, which have no strong features of their own in this wavelength region and were observed near in time to and at similar air mass as the PPNs. These were then multiplied by blackbody functions whose temperatures corresponded to those of the spectral types of the standards and flux-calibrated using the visible–infrared colors, using values given by Tokunaga (2000). The flux calibrations are thought to be accurate to $\pm$30%. Wavelength calibration was achieved using telluric absorption lines and is accurate to about $\pm$0.0001 μm.

Most of the weaker telluric features in the PPN spectra were removed by ratioing. The broad telluric methane absorption feature at 3.32 μm is very strong and difficult to correct for accurately, so we substituted a linear interpolation in the 3.31–3.33 μm portion in most of the final spectra. Some narrow but deep telluric water vapor absorptions also did not ratio out well, due to rapidly varying water vapor column above Mauna Kea on some nights; these and occasional spikes caused by cosmic rays were removed and replaced by interpolated values. Finally, each of the problems enumerated above also contributed in varying degrees to the noncancellation of the many strong telluric features in the 3.2–3.5 μm interval. The remaining spikiness of many of the spectra there is a systematic effect due to these problems, rather than to random noise.

Some of the target objects have been observed previously at lower resolution from the ground using CGS2 ($R \sim 425$) on the 3.8 m United Kingdom Infrared Telescope (UKIRT) and from space using the SWS01 ($R \sim 250$) and PHT-S modes ($R \sim 75$) on the *Infrared Space Observatory* (*ISO*). The use of the larger aperture Keck telescope provided the opportunity to obtain spectra at higher resolution and with higher signal-to-noise ratios (S/N). Previous observations have generally used spectrometer apertures that are much wider than that of our slit ($0.57'' \times 42''$), e.g., CGS2: 5″ diameter; *ISO* SWS01: $14'' \times 20''$; *ISO* PHT-S: $24'' \times 24''$.

3. THE 3 μm SPECTRA

The new 3 μm spectra of these sources are displayed in Figures 1 and 2 in order of central star spectral type (later to earlier, except for IRAS 20000+3239). The spectral types for the PPNs come primarily from Hrivnak (1995) and Hrivnak & Kwok (1999). In all but the hottest two objects (IRAS 01005+7910 and IRAS 21282+5050) the continuum flux density decreases with increasing wavelength. The 3 μm continua in these are due to reddened photospheres, with perhaps small contributions by warm dust. This

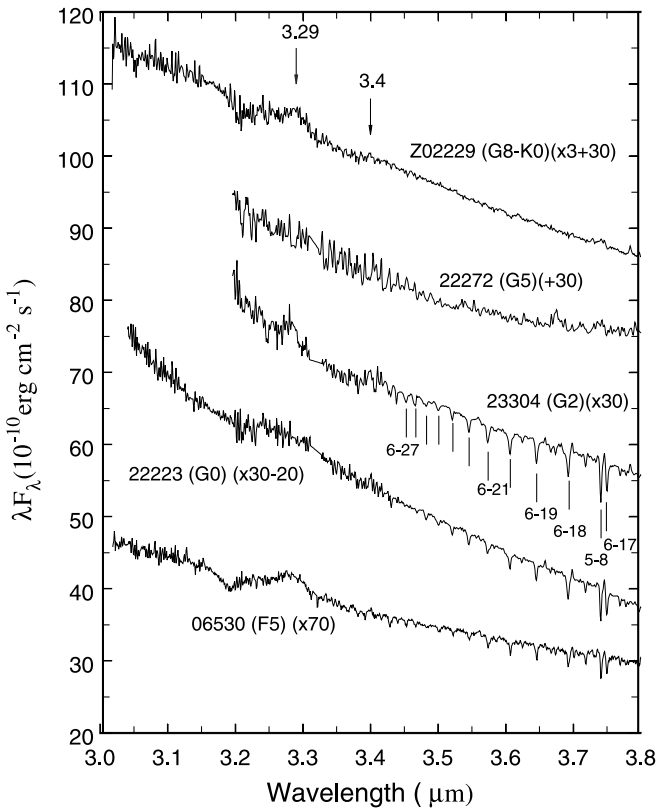

FIG. 1.—Keck NIRSPEC integrated spectra of IRAS Z02229+6208, 22272+5435, 23304+6147, 22223+4327, and 06530−0213. Spectral types and scale factors and offsets of individual spectra are listed. Hydrogen absorption lines are identified in the spectrum of IRAS 23304+6147.

can be seen by examining their visible-infrared spectral energy distributions, which are shown by Hrivnak et al. (2000). We discuss the objects individually below.

IRAS Z02229+6208.—This PPN shows a distinct 3.3 μm emission feature with the suggestion of a weak feature at 3.4 μm. The possible existence of a 3.3 μm feature in the *ISO* SWS01 and PHT-S spectra was mentioned by Hrivnak et al. (2000) but was a marginal detection. The continuum level in the new NIRSPEC data is ~25% lower than the *ISO* spectra but the slope is similar. The difference is at the level of the expected uncertainty in flux levels of the two spectra and thus may or may not be real. It is also possible that some of the difference may be due to the smaller aperture and extended nature of the source. Mid-infrared images of IRAS Z02229+6208 show the central region to have a size (FWHM) of 0.7″, with dust emission extending to 2″ from the central star (Kwok et al. 2002), although the near-infrared emission may be more compact.

IRAS 22272+5435 (=*HD 235858*).—The NIRSPEC spectrum of this object is particularly noisy from 3.2 to 3.5 μm. We found no emission features in the spectrum of the central eight rows (1.50″), as is seen in Figure 1. However, previously both the 3.3 μm and 3.4 μm features had been detected in a ground-based CGS2 spectrum obtained in 1990 (Geballe et al. 1992) and can be seen in *ISO* archival spectra. The difference can be understood in light of the results of Goto et al. (2003) who obtained spatially-resolved 3 μm spectroscopy of IRAS 22272+5435. They found that spectra at the position of the central star do not show the emission features, but that the features are present in spectra at distances from the central star of 0.35″–0.8″ (with the slit oriented along the direction of the infrared enhancement

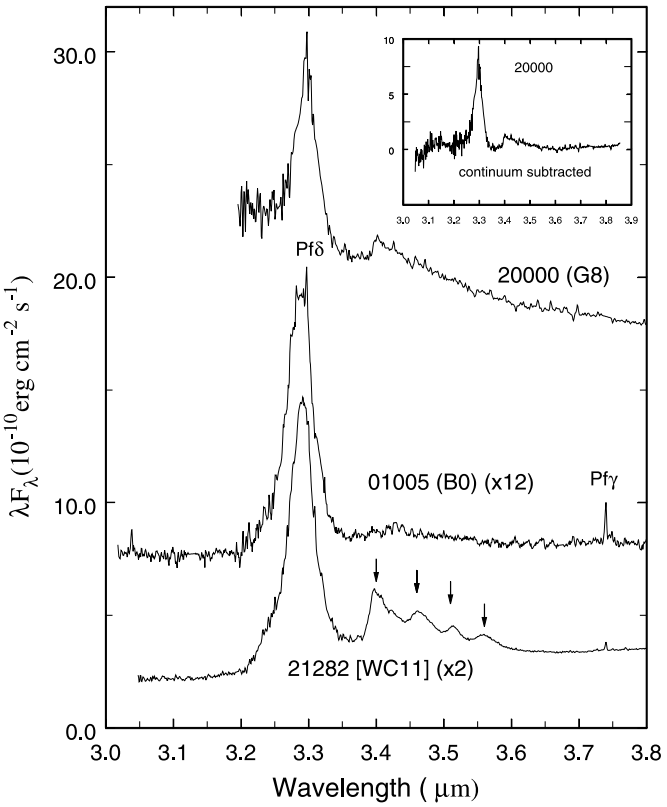

FIG. 2.—Keck NIRSPEC integrated spectra of IRAS 20000+3239, 01005+7910, and 21282+5050. Spectral types and scale factors of individual spectra are listed. Hydrogen Pfund lines are identified. Locations of AIB satellite features in IRAS 21282+5050 are denoted by arrows. The inset shows the continuum-subtracted spectrum of IRAS 20000+3239; the continuum was fitted by two black bodies of $T = 4800$ K and $T = 500$ K.

found by Ueta et al. [2001]). The size of the nebula is $\sim 2''$ at 10 μm and in the visible (Ueta et al. 2000, 2001). The NIRSPEC spectrum of the outer four rows of the initial eight (two rows on each side of the central star) displayed in Figure 3 indeed shows weak 3.3 and 3.4 μm features, with relative strengths similar to those found by Goto et al. (2003). These features were too weak to be seen relative to the strong continuum in the central region when all eight rows were included. These outer rows correspond to an angular distance from the central star of $0.4''$–$0.8''$, or a linear distance of 700–1400 AU at an assumed distance of 1.8 kpc (Volk et al. 2002; for $L = 8300\ L_\odot$).

IRAS 23304+6147.—This PPN shows a weak 3.3 μm emission feature and a marginally detected 3.4 μm feature. In addition, a number of hydrogen absorption lines of the Humphreys series (6–n) are seen between 3.45 and 3.75 μm, along with the Pfγ (5–8) line. This is the first report of the 3.3 μm feature in IRAS 23304+6147. However, a review of the archival *ISO* SWS01 and PHT-S data for this object, which are of a much lower S/N, shows a marginal detection of the 3.3 μm feature and no detection of the 3.4 μm feature. The continuum level in the new NIRSPEC data is $\sim$40% lower than the *ISO* spectra, but the slope is similar. This reduced flux may be due to photospheric variability, pointing errors, or extended faint emission.

IRAS 22223+4327.—The integrated spectrum of this object contains marginal evidence for the 3.3 μm feature and no evidence for the 3.4 μm feature. However, similar to IRAS 22272+5435, the 3.3 μm feature is clearly seen when only the faint spectrum at angular distances of $0.4''$–$0.8''$ (1800–3600 AU at $d =$ 4.8 kpc [Kwok et al. 1995; for $L = 8300\ L_\odot$]) on each side of the central star is extracted. This is shown in Figure 4. The 3.4 μm feature is not seen at the position of the star or in the nebula; thus, these observations appear to refute the claim of a 3.4–3.5 μm emission feature in this object as listed by Bakker et al. (1997). Hydrogen absorption lines are seen in the NIRSPEC spectrum, similar to those seen in IRAS 23304+6147. This is not surprising, since strong hydrogen Brackett absorption lines are present in the *H*-band spectrum (Hrivnak et al. 1994).

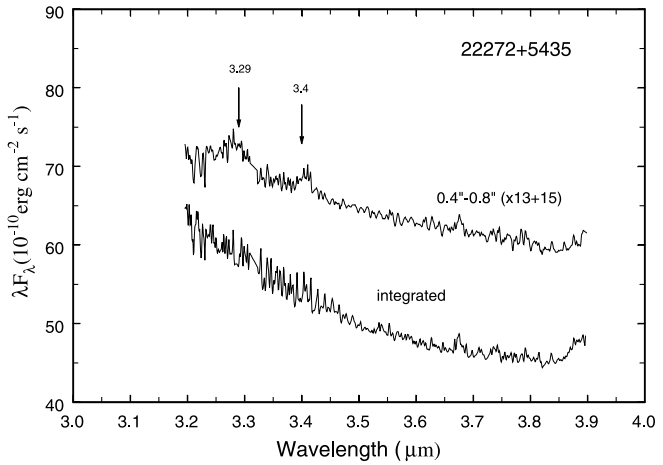

FIG. 3.—Comparison of spectrum of the outer portions ($0.4''$–$0.8''$ on opposite sides of the star) with the integrated spectrum of IRAS 22272+5435. Scale factor and offset of the outer spectrum are listed.

IRAS 06530−0213.—The spectrum, the first of this source in the 3 μm region, shows the 3.3 μm feature but no 3.4 μm feature. Hydrogen absorption lines are also seen, presumably from the photosphere of the F5 star. The nebula has a size of $\sim 2''$ in visible light, oriented approximately north–south (Ueta et al. 2000), but due to contamination of the spectrum by dust on the dewar window, we cannot determine the extent of the AIB emission. A weak absorption feature, which we do not identify, is apparent near 3.19 μm, close in wavelength to a similar feature present in the spectrum of the PPN IRAS 22272+5435 obtained by Goto et al. (2003).

IRAS 20000+3239.—This PPN has a strong 3.3 μm feature and a clear 3.4 μm feature, as is seen in Figure 2. The 3.3 μm feature was first observed in the *ISO* SWS01 and PHT-S data (Hrivnak et al. 2000). The 3.4 μm feature is a new detection. The continuum in the NIRSPEC spectrum is higher than the *ISO* spectrum by

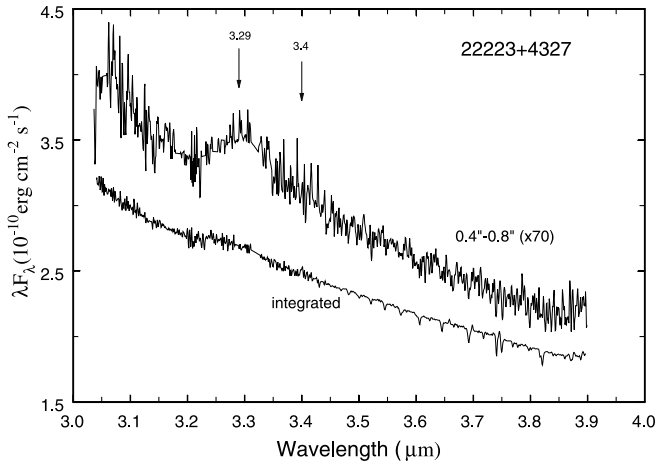

FIG. 4.—Comparison of the outer ($0.4''$–$0.8''$) and integrated spectra of IRAS 22223+4327. The scale factor of the outer spectrum is listed.

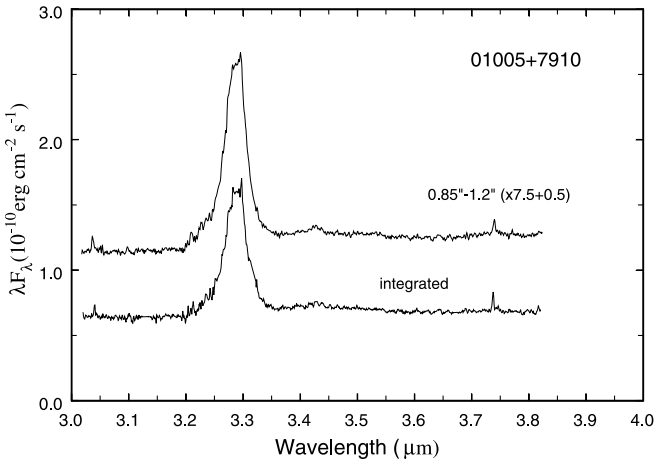

FIG. 5.—Comparison of the outer (0.85″–1.2″) and integrated spectra of IRAS 01005+7910. The scale factor and offset of the outer spectrum are listed.

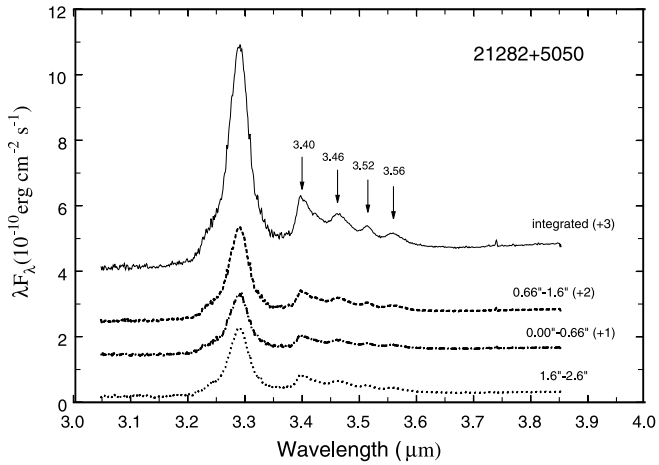

FIG. 6.—Comparison of spectra from the outer (1.6″–2.6″), middle (0.66″–1.6″), and central (0.00″–0.66″) parts of IRAS 21282+5050, along with an integrated spectrum (0.0″–2.6″). The values of the numerical offsets are also listed with each.

~60%. The difference may be due to the poor weather during observations affecting the calibration and/or possibly also to the intrinsic infrared variability of the star, which reaches 0.6 mag in V (Hrivnak et al. 2001).

The spectrum shown in Figure 2 was extracted from 11 rows (2.1″), because NIRSPEC was somewhat out of focus during this observation. To search for spatial variations, we extracted the spectrum from the outer four rows, at a distance of 0.7″–1.0″ on each side of the star. The spectrum of the outer region looks exactly the same as the entire integrated spectrum, but is a factor of 13 fainter, suggesting that the source was unresolved.

IRAS 01005+7910.—This object showed obvious extension in our spectrum and we extracted 13 rows (2.5″). The spectrum shows a very strong 3.3 μm feature and a weak 3.4 μm feature. In addition, the hydrogen emission (recombination) line of Pfγ at 3.741 μm (8–5) is present, as probably is Pfδ at 3.297 μm (9–5). The 3.3 μm feature was first discovered in the *ISO* data (Hrivnak et al. 2000), but this is the first detection of the 3.4 μm feature. The NIRSPEC and *ISO* spectra both show nearly flat continua with similar flux levels. However, the strength of the 3.3 μm feature in the NIRSPEC spectrum is only ~40% of that seen in the *ISO* spectrum. This must be due to the smaller NIRSPEC aperture.

To search for spatial variation, we extracted the outer four rows, thus examining the sum of two regions 0.85″–1.2″ (3100–4500 AU at $d = 3.7$ kpc [Hrivnak et al. 2000; for $L = 8300\ L_{\odot}$]) on each side of the star. This spectrum is shown in Figure 5. Compared to the integrated spectrum, the equivalent widths of the 3.3 and 3.4 μm features are larger, while the equivalent width of Pfγ is similar. Thus, the AIB features are more concentrated in the outer parts of the nebula compared to the continuum and recombination lines.

IRAS 21282+5050.—This object is not a PPN, but rather a young PN with a [WC11] central star. It is obviously extended, as was known from previous imaging (size 6″ × 5″ at 3.3 μm; Meixner et al. 1993), and we began by extracting the spectrum from 23 rows (4.4″). The object is already known to have 3.3 and 3.4 μm features, as well as additional emission feature at 3.46, 3.52, and 3.56 μm (de Muizon et al. 1986; Nagata et al. 1988; Jourdain de Muizon et al. 1990). These are all clearly seen in the new spectrum (see Fig. 2). Also seen in the NIRSPEC spectrum is the hydrogen Pfγ emission line discussed above for IRAS 01005+7910. A 3 μm *ISO* spectrum of this source has been published by Molster et al. (1996).

We tested for spatial variation by extracting the spectrum in three regions of the extended nebula, at projected distances on opposite sides of the star of 0.00″–0.66″, 0.66″–1.6″, and 1.6″–2.6″. These correspond to linear distances of 0–2300, 2300–5700, and 5700–9200 AU, respectively, at $d = 3.5$ kpc (Kwok et al. 1993; for $L = 8300\ L_{\odot}$). The resulting spectra are shown in Figure 6, along with the integrated spectrum. There is no significant change in the profiles or relative strengths of the features with distance from the star.

4. DISCUSSION

4.1. 3.3 *and* 3.4 μm *Features*

A summary of the 3.3 and the 3.4 μm emission features observations in carbon-rich PPNs is given in Table 2. Included are the present targets and previous observations of others. The 3 μm survey of carbon-rich PPNs is now essentially complete. We had initially hoped to detect the 3.4 μm feature in several more of our target PPNs at high enough S/N that we could obtain accurate profiles of the feature and compare them among themselves and to the 3.4 μm feature in PNs. However, in almost all cases the 3.4 and even the 3.3 μm features, where detected, are weak, and the spectra are mainly useful for detection purposes only. The only exceptions to this are the newly detected 3.4 μm feature in IRAS 20000+3239 and the previously detected 3.3 μm features in IRAS 20000+3239 and IRAS 01005+7910. In a few cases we and others have found that the AIB emission is extended. However, except for the two cases in which we detected extended and spatially-varying emission, IRAS 22272+5435 and 22223+4327, the spectra in Figures 1 and 2, which sample rectangular regions of dimension 0.57″ × 1.5″–2.5″, are presumably representative of the total 3 μm spectra of each of these PPNs. This is not to say that the AIB emission in the other sources we observed is not also extended, but only that our angular resolution was insufficient to resolve them.

With the exception of IRAS 22272+5435, the profiles of the 3.3 μm features and, where detected, the 3.4 μm features in the PPN spectra in Figures 1, 2, and 4 resemble those of typical carbon-rich planetary nebulae, i.e., the "Class A" spectra as described in Geballe (1997). They clearly are not similar to the "Class B" features that have been found in a few PPNs, because the 3.4 μm features are neither comparable in strength to the 3.3 μm features nor as broad as the Class B 3.4 μm features and because in many cases the sharp leading edge characteristic of the Class A 3.4 μm

TABLE 2

SUMMARY OF THE PRESENCE OF THE 3.3 AND 3.4 μm EMISSION FEATURES AND OTHER CORRELATED FEATURES IN CARBON-RICH PPNs

Object	Spectral Type	3.3	3.4	Class A/B[a]	References	21 μm[b]	C_2[c]	C_3[c]	C/O[d]
Z02229+6208	G8–K0 0–Ia	Y	Y:*	A	1	Y	Y	Y	...
20000+3239	G8 Ia	Y	Y*	A	1	Y	Y	...	...
05113+1347	G8 Ia	Y:	Y:	...	2	Y	Y	Y	2.4
22272+5435	G5 Ia	Y	Y	B	1, 3, 4	Y	Y	Y	1.6
07430+1115	G5 0–Ia	Y	Y	A	5	N:	Y	Y	...
23304+6147	G2 Ia	Y*	Y:*	A	1	Y	Y	Y	2.8
05341+0852	G2 0–Ia	Y	Y	B	6	Y	Y	Y	1.6
22223+4327	G0 Ia	Y	N	A	1	Y	Y	Y	1.2
04296+3429	G0 Ia	Y	Y	B	3	Y	Y	Y	...
AFGL 2688	F5 Iae	Y	Y	A	3	Y	Y	Y	1.0
06530−0213	F5 I	Y*	N	A	1	Y	Y	Y	2.8
07134+1005	F5 I	Y	Y	A	7	Y	Y	N	1.0
19500−1709	F3 I	N	N	...	8	Y	N	N	1.0
16594−4656	B7	Y	N	A	9	Y	N	N	...
01005+7910	B0	Y*	Y*	A	1	N	N	N	1.2
22574+6609[e]	...	...	...	...	...	Y	...	...	...
19477+2401[e]	...	...	...	...	...	Y	...	...	...

NOTE.—An asterisk (*) indicates a new detection; a colon (:) indicates a marginal or uncertain detection of the emission feature.

[a] Classification scheme of Geballe (1997).

[b] References to the 21 μm feature based on *ISO* spectra are from Volk et al. (1999), Hrivnak et al. (2000), and Volk et al. (2002); and *Spitzer* spectra are from Hrivnak et al. (2006).

[c] References to the presence of C_2 and C_3 features are from Hrivnak (1995), Bakker et al. (1997), and Hrivnak & Kwok (1999).

[d] References to C/O abundances multiple objects: Reddy et al. (2002), van Winckel & Reyniers (2000); IRAS 06530−0213: Reyniers et al. (2004); IRAS 01005+7910: Klochkova et al. (2002); AFGL 2688: Klochkova et al. (2000).

[e] These objects are included, because they share the property of almost all of the other sources of displaying an emission feature at 21 μm. However, they are very faint, $V = 21–22$, and no visible or 3 μm spectra have been obtained for them.

REFERENCES.—(1) This paper; (2) Hrivnak et al. 1994; (3) Geballe et al. 1992; (4) Goto et al. 2003; (5) Hrivnak & Kwok 1999; (6) Geballe & van der Veen 1990; (7) Kwok et al. 1990; (8) ISO archive; (9) García-Lario et al. 1999.

feature (but not of Class B) is present. IRAS 22272+5435 is a prime example of a Class B source (along with IRAS 04296+3429 and 05341+0852; see Geballe 1997; Geballe et al. 1992), and the spatially-resolved spectra of Goto et al. (2003) and this paper show this.

For the PPNs whose spectra are displayed in Figure 1, the 3.3 μm features rise only a few percent above the continuum level, whereas for the PPNs in Figure 2, the feature is 30% above the continuum in the case of IRAS 20000+3239 and twice the continuum for IRAS 01005+7910. The spectra of both of them, as well as that of IRAS 21282+5050, also show the frequently observed "plateau" of AIB emission under the 3.3 and 3.4 μm features, which extends at least to 3.55 μm. The spectral type of the central star of IRAS 01005+7910 is B0, suggesting that it is nearly into the PN stage, and thus, the high equivalent widths of its AIB features are understandable. However, the fairly high equivalent widths of these features in IRAS 20000+3239 seem inconsistent with its well-established spectral classification of G8 Ia (Hrivnak 1995) and are indeed highly unusual in a star with a late spectral type. Unless it contains a hot companion that might be exciting the feature, for which there is no evidence, the strength of the 3.3 μm feature in this object is a challenge to the current understanding of the excitation of Class A and B features. Another example of this phenomenon, albeit in a somewhat hotter object, is AFGL 2688 (the Egg Nebula), a carbon-rich PPN with an F5 Iae central star and a strong 3.3 μm feature (Geballe et al. 1992).

In addition to the more prominent emission features at 3.3 and 3.4 μm, satellite features at 3.46, 3.52, and 3.56 μm are present in the spectrum of IRAS 21282+5050. The spectrum of this source has previously been regarded as Class A (Geballe 1997), with these weaker features being more prominent in IRAS 21282+5050 than in other Class A spectra. The identities of the satellite features are generally regarded as $-CH_2$, $-CH_3$, and other aliphatic side groups on hydrocarbons (de Muizon et al. 1986; Geballe et al. 1989; Jourdain de Muizon et al. 1990), although specific molecular species have not been identified.

4.2. *Correlations of the* 3.3 *and* 3.4 μm *Features with Other Properties*

From this essentially complete survey of carbon-rich PPNs, we find that there is not a simple correlation between the appearance of the 3 μm AIBs and spectral type. For the most part the Class A AIBs strengthen with earlier spectral type, but there are notable exceptions to this trend. IRAS 20000+3239 is perhaps the most blatant example, but there are others as well (e.g., AFGL 2688 and IRAS 06530−0213 have similar spectral type central stars but very different 3 μm spectra). Moreover, several PPNs possess the Class B features, which differ strikingly from the more common Class A features, suggesting that a different chemistry is occurring in them. Thus, factors other than spectral type must affect the 3 μm band emission feature strengths, profiles, and intensity ratios during the PPN stage, such as carbon abundance, dust mass, binarity (especially if a hot compact companion were to be present), and perhaps geometry of the circumstellar envelope.

To explore some of these other factors and possibly reveal correlations, we have included in Table 2 an indicator of the presence of the 21 μm emission feature and of molecular carbon (C_2 and C_3) and also the carbon-to-oxygen ratio where these values are available. Almost all of the sources have either a direct measurement of C/O ≥ 1 or the presence of C_2, and they are thus classified as carbon-rich. The only sources for which this is not the case is the hot object IRAS 16594−4656, which does not

have a high-resolution spectroscopic abundance study but which has AIB features (García-Lario et al. 1999; Hrivnak et al. 2000), and the faint objects IRAS 17477+2401 and 22574+6609, which are described below. Several of the sources without C/O values are observed to be enriched in carbon but do not have accurate oxygen abundance measurements. The two Class B objects with observed C/O abundances fall in the middle of the observed C/O range and thus there does not appear to be a correlation between Class B and the C/O value.

Almost all of the sources exhibit the 21 μm emission feature. While the carrier of this feature is not yet clearly identified, most suggestions involve carbon (see Speck & Hofmeister 2004 and references therein) since these sources are known to be carbon-rich. The only sources in this table without an observed 21 μm feature are IRAS 07430+1115, which does not have an *ISO* or *Spitzer* spectrum, and IRAS 01005+7910, which has the hottest central star. Without trying to explain the cause of the absence in IRAS 01005+7910, which is outside the scope of the present study, we can simply point out the correlation of the 21 μm feature and the 3.3 and 3.4 μm features. Note that we have included for completeness in Table 2 all of the 21 μm sources, even IRAS 22574+6609 and 19477+2401, which are faint, with *V*-magnitudes of 21 and 22, respectively (Su et al. 2001), and which lack both 3 μm spectra and chemical abundance studies.

Included in Table 2 is IRAS 19500−1709, which is carbon-rich, but does not show the 3.3 μm feature in the only available 3 μm spectrum, which is from the *ISO* archives. Before assuming that this feature is missing, it would be prudent to obtain a spectrum at a higher S/N.

4.3. *Hydrogen Lines*

Absorption lines of hydrogen, including Pfγ (5–8, 3.741 μm) and numerous lines from the Humphreys (6–n) series are present in the spectra of IRAS 23304+6147, 22223+4325, and 06530−0213 (Fig. 2), whose spectral classifications are early G to mid F. The strengths of these absorption lines attest to the highly extended photospheres of these post-AGB stars. In F and G dwarfs the Humphreys series lines are not detected at this spectral resolution, and Pfγ is far weaker (Vandenbussche et al. 2002). Not surprisingly, these lines are not seen in the cooler photospheres of the three late-G PPNs whose spectra are shown in Figures 1 and 2. Hydrogen recombination emission lines (Pfγ, Pfδ) are seen in the spectra of the two hot objects, IRAS 01005+7910 and IRAS 21282+5050.

5. SUMMARY AND CONCLUSIONS

1. The 3.3 μm emission feature is detected in all seven PPNs observed in this study, with three being new discoveries and one a confirmation of a previous marginal result.

2. The 3.4 μm emission feature is detected in three of the observed PPNs, two being new discoveries and one a confirmation of a previous marginal result, with two additional possible detections.

3. In IRAS 22272+5435, the 3.3 and 3.4 μm features are found to be spatially extended and seen in the nebula offset from the star, but not at the location of the central star, consistent with the observation of Goto et al. (2003). A similar result is found for the 3.3 μm feature in IRAS 22223+4327.

4. In all of the sources observed in this study except IRAS 22272+5435, the AIB features can be classified as Class A, with the 3.3 μm feature much stronger than the 3.4 μm feature.

5. No correlation is found between the relative strength of the 3.3 and 3.4 μm emission features and the spectral type of the central star, even though the range is G8–B0 (albeit with only one object observed in this study hotter than F5). There are several examples of objects with similar spectral type central stars and very different 3.3 and 3.4 μm feature strengths and relative ratios, such as IRAS 05113+1347 and 20000+3239, both G8 Ia, and IRAS 06530−0213 and AFGL 2688, both F5 Ia.

6. A correlation is observed between the presence of the 3.3 and 3.4 μm emission features and both a carbon-rich nature, as expected, and the presence of the 21 μm emission feature (except IRAS 01005+7919).

7. The distinction between Class A and Class B 3 μm features is not correlated with the C/O value.

We thank Kevin Volk very much for help with the *ISO* spectra, Marianne Takamiya for help in carrying out the observations, and the anonymous referee for detailed comments that helped to improve this paper. This work was supported by grants to B. J. H. from the National Science Foundation (9900846, 0407087) and to S. K. from the Natural Science and Engineering Research Council of Canada. T. R. G.'s research is supported by the Gemini Observatory, which is operated by the Association of Universities for Research in Astronomy, Inc., on behalf of the international Gemini partnership of Argentina, Australia, Brazil, Canada, Chile, the United Kingdom, and the United States of America.

REFERENCES

Allamandola, L. J., Tielens, A. G. G. M., & Barker, J. R. 1989, ApJS, 71, 733
Bakker, E. J., van Dishoeck, E. F., Waters, L. B. F. M., & Schoenmaker, T. 1997, A&A, 323, 469
de Muizon, M., Geballe, T. R., d'Hendecourt, L. B., & Baas, F. 1986, ApJ, 306, L105
Duley, W. W., & Williams, D. A. 1981, MNRAS, 196, 269
———. 1983, MNRAS, 205, 67P
Forrest, W. J., Houck, J. R., & McCarthy, J. F. 1981, ApJ, 248, 195
García-Lario, P., Manchado, A., Ulla, A., & Manteiga, M. 1999, ApJ, 513, 941
Geballe, T. R. 1997, in ASP Conf. Proc. 122, From Stardust to Planetesimals, ed. Y. J. Pendleton & A. G. G. M. Tielens (San Francisco: ASP), 119
Geballe, T. R., Tielens, A. G. G. M., Allamandola, L. J., Moorhouse, A., & Brand, P. W. J. L. 1989, ApJ, 341, 278
Geballe, T. R., Tielens, A. G. G. M., Kwok, S., & Hrivnak, B. J. 1992, ApJ, 387, L89
Geballe, T. R., & van der Veen, W. E. C. J. 1990, A&A, 235, L9
Goto, M., et al. 2003, ApJ, 589, 419
Guillois, O., Nenner, I., Papoular, R., & Reynaud, C. 1996, ApJ, 464, 810
Hony, S., Waters, L. B. F. M., & Tielens, A. G. G. M. 2002, A&A, 390, 533
Hrivnak, B. J. 1995, ApJ, 438, 341
Hrivnak, B. J., & Kwok, S. 1999, ApJ, 513, 869
Hrivnak, B. J., Kwok, S., & Geballe, T. R. 1994, ApJ, 420, 783
Hrivnak, B. J., Volk, K., & Kwok, S. 2000, ApJ, 535, 275
———. 2006, BAAS, 38, 1029
Hrivnak, B. J., et al. 2001, in Post-AGB Objects as a Phase of Stellar Evolution, ed. R. Szczerba & S. K. Górny (Dordrecht: Kluwer), 101
Imanishi, M., & Dudley, C. C. 2000, ApJ, 545, 701
Joblin, C., Tielens, A. G. G. M., Allamandola, L. J., & Geballe, T. R. 1996, ApJ, 458, 610
Jourdain de Muizon, M., d'Hendecourt, L. B., & Geballe, T. R. 1990, A&A, 235, 367
Klochkova, V. G., Szczerba, R., & Panchuk, V. E. 2000, Astron. Lett., 26, 439
Klochkova, V. G., Yushkin, M. V., Miroshnichenko, A. S., Panchuk, V. E., & Bjorkman, K. S. 2002, A&A, 392, 143
Kwok, S. 1993, ARA&A, 31, 63
Kwok, S., Hrivnak, B. J., & Geballe, T. R. 1990, ApJ, 360, L23
———. 1995, ApJ, 454, 394
Kwok, S., Hrivnak, B. J., & Langill, P. P. 1993, ApJ, 408, 586
Kwok, S., Volk, K., & Bernath, P. 2001, ApJ, 554, L87
Kwok, S., Volk, K., & Hrivnak, B. J. 1989, ApJ, 345, L51
———. 1999, A&A, 350, L35
———. 2002, ApJ, 573, 720

Léger, A., & Puget, J. L. 1984, A&A, 137, L5
Lequeux, J., & Jourdain de Muizon, M. 1990, A&A, 240, L19
Li, A., & Draine, B. T. 2002, ApJ, 572, 232
McLean, I. S., et al. 1998, Proc. SPIE, 3354, 566
Meixner, M. et al. 1993, ApJ, 411, 266
Molster, F. J., et al. 1996, A&A, 315, L373
Nagata, T., Tokunaga, A. T., Sellgren, K., Smith, R. G., & Sakata, A. 1988, ApJ, 326, 157
Omont, A., et al. 1995, ApJ, 454, 819
Papoular, R. 2001, A&A, 378, 597
Papoular, R., Conard, J., Guillois, O., Nenner, I., Reynaud, C., & Rouzaud, J.-N. 1996, A&A, 315, 222
Pendleton, Y. J., & Allamandola, L. J. 2002, ApJS, 138, 75
Pendleton, Y. J., Sandford, S. A., Allamandola, L. J., Tielens, A. G. G. M., & Sellgren, K. 1994, ApJ, 437, 683
Puget, J. L., & Léger, A. 1989, ARA&A, 27, 161
Reddy, B. E., Lambert, D. L., Gonzalez, G., & Young, D. 2002, ApJ, 564, 482
Reyniers, M., van Winckel, H., Gallino, R., & Straniero, O. 2004, A&A, 417, 269
Sakata, A., Wada, S., Tanabé, T., & Onaka, T. 1984, ApJ, 287, L51
Speck, A. K., & Hofmeister, A. M. 2004, ApJ, 600, 986
Su, K. Y. L., Hrivnak, B. J., & Kwok, S. 2001, AJ, 122, 1525
Tokunaga, A. T. 2000, in Allen's Astophysical Quantities, ed. A. N. Cox (New York: Springer), 143
Ueta, T., Meixner, M., & Bobrowsky, M. 2000, ApJ, 528, 861
Ueta, T., et al. 2001, ApJ, 557, 831
Vandenbussche, B., et al. 2002, A&A, 390, 1033
van Winckel, H., & Reyniers, M. 2000, A&A, 354, 135
Volk, K., Kwok, S., & Hrivnak, B. J. 1999, ApJ, 516, L99
Volk, K., Kwok, S., Hrivnak, B. J., & Szczerba, R. 2002, ApJ, 567, 412
Volk, K., Xiong, G.-Z., & Kwok, S. 2000, ApJ, 530, 408